

The growth of InN and related alloys by high-pressure CVD

Nikolaus Dietz^{*a}, Mustafa Alevli^a, Hun Kang^b, Martin Straßburg^a, Vincent Woods^a, Ian T. Ferguson^b, Craig E. Moore^d and Beatriz H. Cardelino^c

^a Department of Physics and Astronomy, Georgia State University, Atlanta, GA 30302

^b School of Electrical and Computer Eng., Georgia Institute of Technology, Atlanta, GA 30332

^c Space Sciences Laboratory, NASA Marshall Space Flight Center, Huntsville, AL 35812

^d Chemistry Department, Spelman College, Atlanta, GA 30314

ABSTRACT

The growth of high-quality InN and indium rich group III-nitride alloys are of crucial importance for the development of high-efficient energy conversion systems, THz emitters and detectors structures, as well as for high-speed linear/nonlinear optoelectronic elements. However, the fabrication of such device structures requires the development of growth systems with overlapping processing windows in order to construct high-quality monolithic integrated device structures. While gallium and aluminum rich group III-nitrides are being successfully grown by organometallic chemical vapor deposition (OMCVD), the growth of indium rich group III-nitrides presents a challenge due to the high volatility of atomic nitrogen compared to indium. In order to suppress the thermal decomposition at optimum processing temperatures, a new, unique high-pressure chemical vapor deposition (HPCVD) system has been developed, allowing the growth of InN at temperatures close to those used for gallium/aluminum-nitride alloys.

The properties of InN layers grown in the laminar flow regime with reactor pressures up to 15 bar, are reported. Real-time optical characterization techniques have been applied to analyze gas phase species and are highly sensitive the InN nucleation and steady state growth, allowing the characterization of surface chemistry at a sub-monolayer level. The *ex-situ* analysis of the InN layers shows that the absorption edge in the InN shifts below 0.7 eV as the ammonia to TMI precursor flow ratio is lowered below 200. The results indicate that the absorption edge shift in InN is closely related to the In:N stoichiometry.

Keywords: high-pressure CVD, group III-nitrides, thin film growth, InN, real-time optical monitoring

1. INTRODUCTION

Improved group III-nitride materials (e.g. AlN-GaN-InN) will provide the basis for novel devices that are of significant importance to space exploration missions due to their robustness against radiation damage. Device structures based on $(\text{Ga}_{1-y-x}\text{Al}_y\text{In}_x)\text{N}$ heterostructures and related alloys will enable the fabrication of

- *high-efficient energy conversion systems (multi-tandem solar cells & solid state lighting),*
- *high speed optoelectronics for optical communication systems,*
- *solid state lasers operating in the blue and ultraviolet regions,*

* Email: ndietz@gsu.edu

- *spintronic and Terahertz device structures, and*
- *nonlinear optical switching elements based on photonic band gap structures.*

Large-area/scale growth of group III-V semiconductor device structures has been proven most efficient by organometallic chemical vapor deposition (OMCVD - also denoted as MOVPE)¹. It also has been successfully applied to the growth of (Ga_{1-y}Al_y)N device structures^{2,3}. However, the growth of indium rich (In_{1-x}Ga_x)N by low-pressure OMCVD becomes a major challenge due to stoichiometric instabilities and low dissociation temperatures, leading to inconsistent and process dependent materials properties. The considerable uncertainty over the band gap of InN, the influence of the intrinsic materials point defect chemistry on the optical and electrical properties^{4,5}, and the effect of extrinsic impurities such oxygen on the band gap show the lack of understanding for even the binary InN system. At present, the band gap values for MBE grown InN layers grown in the process window of about 480-550°C are reported at approximately 0.7 eV with carrier concentration as low as $n_e = 10^{17} \text{ cm}^{-3}$. The current status of InN growth and characterization are presented in controversial reviews provided^{5,6,7,8,9}, implying that different approaches for the growth of In-rich group-III-nitride alloys need to be explored in order to improve the structural and optical properties of InN and related alloys.

In order to stabilize indium-rich compounds at growth temperatures similar to those employed for AlN-GaN alloys, a unique high-pressure chemical vapor deposition (HPCVD)^{10,11} system has been developed, demonstrating the successful suppression of the InN decomposition for growth temperatures well above 1100 K. This is a major step toward the growth of indium rich group III-nitride alloys and heterostructures, since such growth temperatures are close to those used for (Ga_{1-y}In_y)N. The move toward high-pressure CVD adds the additional flexibility of controlling the vapor pressures of the constituents on the growth surface. The challenging path, however, is the increased complexity that requires consideration of gas flow dynamics and gas phase reactions.¹² In order to study the gas phase and surface chemistry processes involved, real-time optical monitoring techniques^{13,14} are integrated in the HPCVD system for the characterization of gas flow, gas phase decomposition kinetics, as well as surface reactions, which are crucial in order to gain insights in the growth process and in order to control the process on a sub-monolayer level. Provisions are implemented to address the control of gas phase reactions, extracting sufficient organometallic (OM) nutrients from the OM-bubblers, and embedding the precursor flows in the reactor main stream. The InN growth results discussed below are limited to the laminar flow regime for the HPCVD reactor.

2. EXPERIMENT

A high-pressure flow channel reactor with incorporated real time optical characterization capabilities is utilized to study and optimize InN nucleation and growth¹⁰. Ammonia (NH₃) and trimethylindium (TMI) are employed in a pulsed injection scheme, schematically depicted in Fig. 1. The cycle sequence time is varied from 4 sec to 8 sec, with TMI and ammonia pulse widths from 0.3-0.6sec and 0.8-1.5 sec, respectively. The pulsed precursors are embedded and temporally controlled in a high pressure carrier stream, consisting of ultra-pure nitrogen, supplied from boil-off liquid nitrogen. A point-of-use “nanochem” purifier is used in the ammonia supply line in order to reduce oxygen contamination. The total gas flow through the reactor as well as the reactor pressure are kept constant at all times. Optical access ports along the center axis of the substrates, perpendicular to the gas flow direction, are used to monitor the gas flow kinetics and gas phase reactions via ultraviolet absorption spectroscopy (UVAS). The growth surface is monitored through the back side of the

sapphire substrate, utilizing principal angle reflectance spectroscopy (PARS)¹⁵ and laser light scattering (LLS). For the growth results presented here, the reactor pressure was varied between 10 bar and 15 bar, and gas flows from 2 slm to 12 slm, maintaining laminar flow conditions¹³. The precursor flow ratio are evaluated for molar ratio ammonia to TMI, $R_{\text{NH}_3 : \text{TMI}}$, from 200 to 1000 in the growth temperature regime of 900 K to 1150 K. All temperatures settings refer to the calibrated correlation of the analyzed black body radiation as a function of the power setting of the substrate heater. Note, that the actual gas phase temperatures and the growth surface temperatures are strongly influenced by the gas flow velocity (total main flow) and the surface emissivity. No corrections for these effects are provided at present.

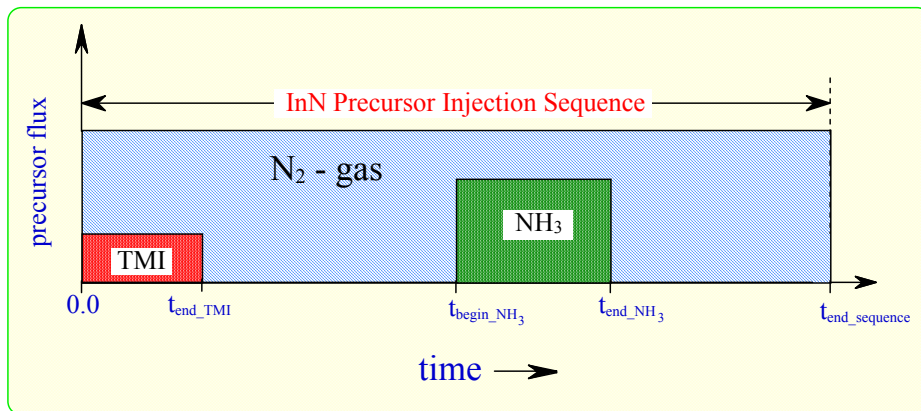


Figure 1
Schematic representation of a precursor cycle sequence used for the growth of InN via the precursors TMI and ammonia in a high pressure ambient.

3. RESULTS AND DISCUSSION

3.1. Real-time optical characterization of InN nucleation and growth

Decomposition studies of the ammonia precursor¹⁴ indicate an onset of ammonia decomposition at temperatures above 900 K. These studies also show that the observed onset in the ammonia decomposition decreases with increasing reactor pressure. The InN nucleation and growth process are monitored by PARS and LLS. Figure 2 shows typical PARS and LLS traces recorded for the wavelength $\lambda=632.8$ nm during InN growth under HCVD conditions. The reactor pressure is maintained at 11 bar and the gas flow velocity is estimated at 43 cm/s. The ammonia to TMI molar ratio is 8000. A cycle sequence of 6s and a precursor pulse separation of 0.6s are used. As depicted in Fig. 2, the PARS signal exhibit two components: a) an oscillation related to the overall film growth, expressed through the large-scale interference fringes, and b) a fine structure (as resolved in more detail in Fig. 3) that strongly correlates to the time sequence of the supply of precursors employed, providing information on the growth surface chemistry and kinetics. The strong damping of the interference fringes indicate the presence of absorption at the monitored wavelength which leads to a loss in surface sensitivity after prolonged growth. The temporal evolution of the LLS trace indicates that the surface roughness during growth remains low and even slightly decreases. Analysis of the PARS trace provides the average growth rate and the average differences in the dielectric functions between film and substrate.¹⁶

The fine structure, superimposed on the PARS trace, is shown in more detail in the top trace in Fig.

3. Each fine structure oscillation corresponds to a complete precursor cycle sequence, as shown in the pulse sequence. The reduction in the PAR signal correlates to the overall InN film growth process, while the fine structure oscillations correlate to the pulsed precursor exposure as indicated in the UV absorption trace, shown in the lower part of Fig. 3. There is a distinct time-lag between precursor pulse position (opening of valve) and the corresponding optical response. The time lag (see arrows) relates to the average gas velocity and the travel distance between the valve and the monitoring point.¹⁴ The UV gas phase absorption is monitored simultaneously with the PARS signal as depicted in the lower part of Fig. 3. The UV gas phase absorption trace monitors the undecomposed concentration of both precursors, TMI and ammonia, in the gas phase above the growth surface.¹¹ Both the UVAS and PARS trace provide a snapshot of the growth conditions at the center axis of the substrate.

Note that the variation of the process parameters/conditions along the flow direction are not accessible and will require comprehensive flow and reactor modeling. Such a process model will have to include details on the temporal fine structure evolution and the correlation to gas phase constituents as obtained by UVAS which is discussed in earlier publications.¹⁶ PARS is a highly sensitive surface diagnostic tool with sub-monolayer resolution, able to operate at high pressures, illustrated in Fig. 3. Its surface sensitivity enables the tracking of variations in surface constituents, which can be linked to the evolution of precursor species/fragments in the gas phase.

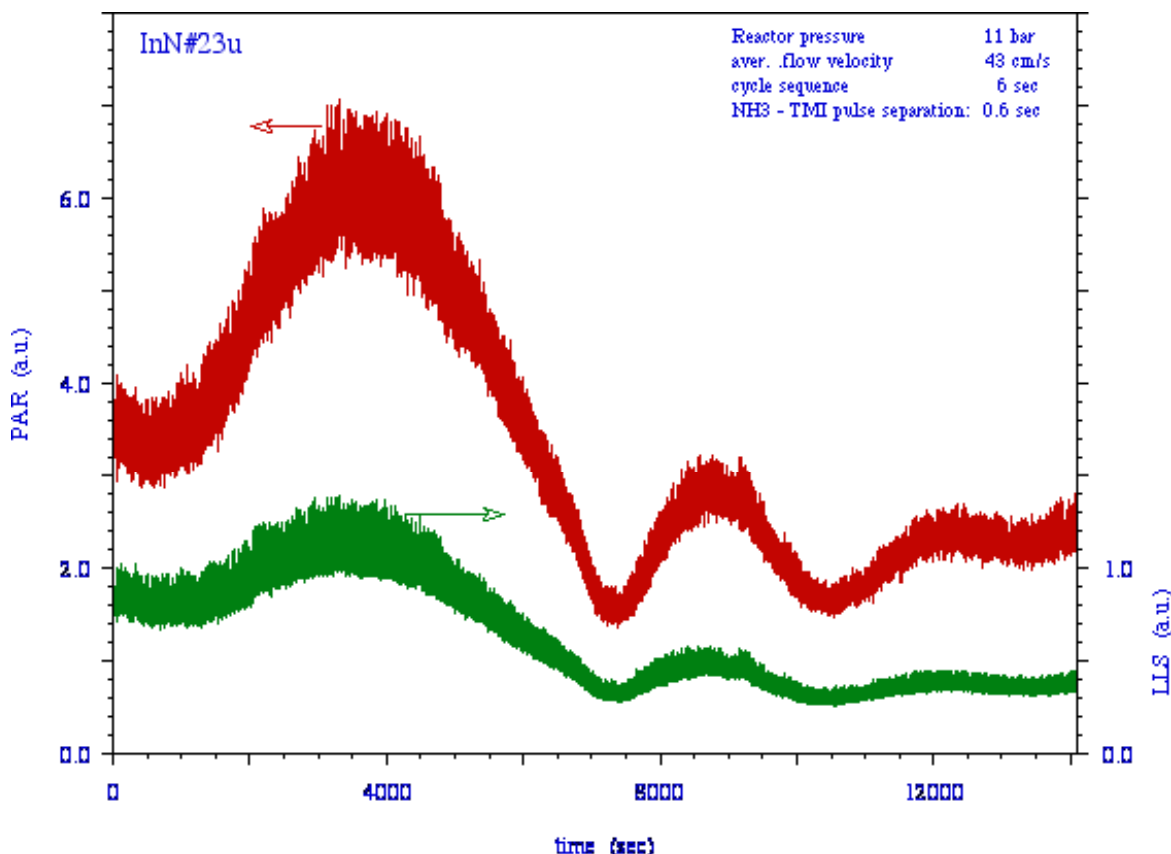


Figure 2: Real-time optical monitoring of InN growth on sapphire (0001) by principal angle reflectance (PAR) and laser light scattering (LLS) using 632.8 nm laser light.

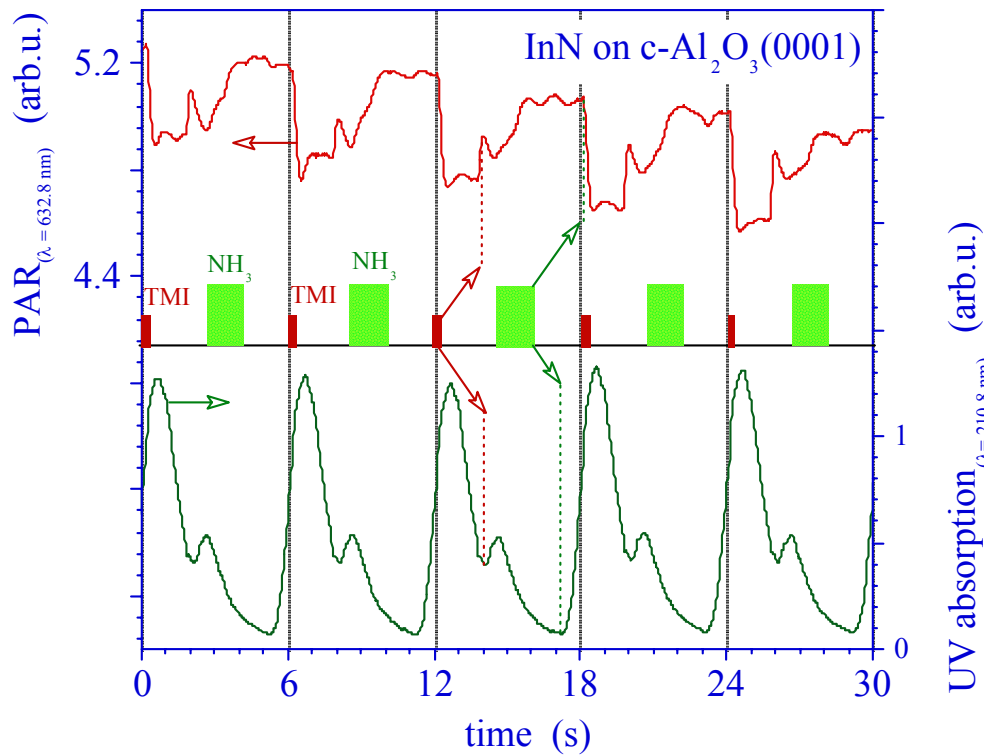


Figure 3:

Top trace: Principal angle reflectance (PAR) fine structure oscillation monitored under steady-state growth conditions using a 6 sec precursor cycle sequence. Bottom trace: UVAS trace monitored at 201.8 nm.

3.2. Ex-situ InN layer characterization

The structural properties of epitaxially grown InN films have been investigated using X-ray diffraction and Raman spectroscopy. Figure 4 depicts the XRD spectra recorded in the θ - 2θ mode for characteristic samples #22U, #24L_A and #25L_C, where the precursor flow ratio $R_{\text{NH}_3:\text{TMI}}$ was systematic lowered from 8000 down to 200. The growth temperature was 850°C, with a reactor pressure of 11 bar and an average gas flow velocity of 45 cm/s. Sample #22U, shows a broad reflection from wurtzite-type InN centered at 31.26 deg with full-width at half-maximum (FWHM) of 650 arcsec. In sample #24L_A, the precursor flow ratio $R_{\text{NH}_3:\text{TMI}}$ is lowered to 1000. Under these conditions the InN (002) reflection is broadened and shifted to 31.2 deg and the InN (101) reflection at 31.1 deg becomes more pronounced. For $R_{\text{NH}_3:\text{TMI}}$ around 200 (sample #25L_C), both InN (002) and InN (101) reflection show double structures, indicating the existence of phases with FWHM's below 200 arcsec in very close proximities. The analysis of the X ray spectra on (102) and (002) reflection planes for the samples #22U and #2L_C provided the lattice constants $a=3.557\text{\AA}$ and $c=5.754\text{\AA}$. These values are quite close to the other reported values of $a=3.548\text{\AA}$ and $c=5.76\text{\AA}$ of Tansley et al.¹⁷, $a=3.544\text{\AA}$ and $c=5.718\text{\AA}$ of Osamura et al.¹⁸, and $c=5.69\text{\AA}$ of Wakahara et al.¹⁹

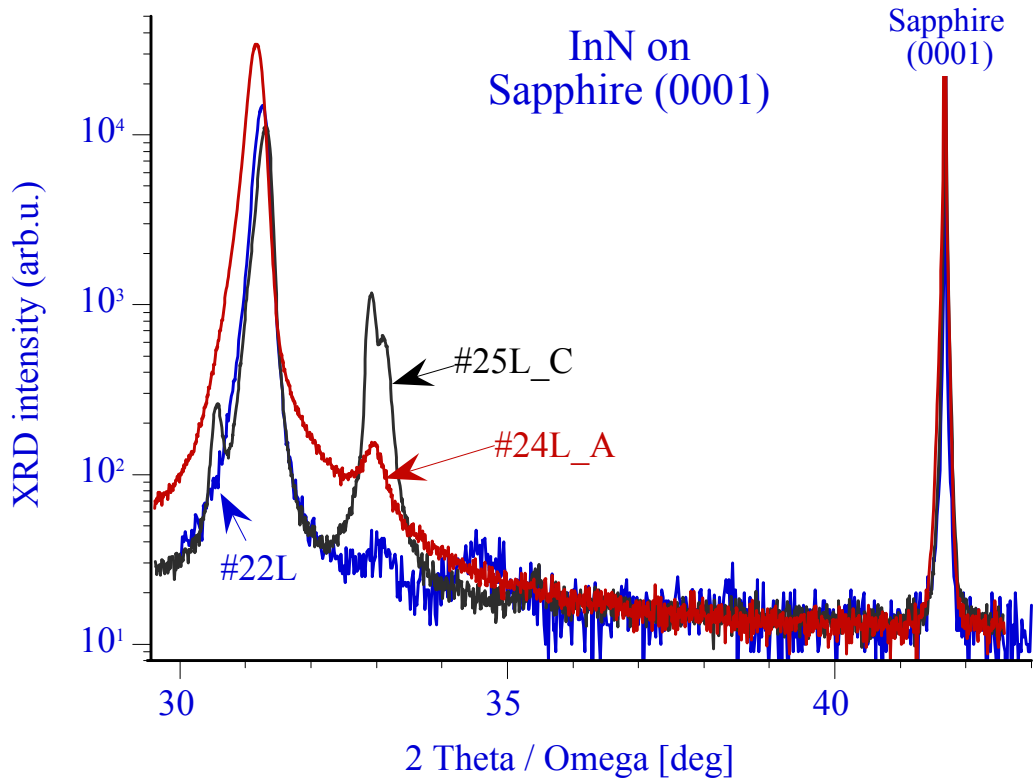


Figure 4: XRD spectra from InN layers grown with precursor flow ratio $R_{\text{NH}_3:\text{TMI}}$ of 8000 (#22L), 1000 (#24L_A) and 200 (#25L_C).

At this point, it can be not excluded that the observed asymmetric line shape for the InN (002) and InN (101) reflections is caused due to the close proximity of Indium oxide (In_2O_3) reflections, which are reported at 30.58 deg for In_2O_3 (222), 33.09 deg for In_2O_3 (321), and 35.54 deg for In_2O_3 (400).²⁰ The appearance of additional phases as seen in sample #25L_C do not match known Indium oxide (In_2O_3) reflections.

Figure 5 shows the absorption spectra observed for a set of characteristic samples #22L, #24L_A, #25L_C, #30L and #31L. Samples #30L and #31L are grown with a $R_{\text{NH}_3:\text{TMI}}$ ratio of 450 and a substrate temperature of 850°C. The reactor pressure was 15 bar with a gas flow velocity of 50 cm/s.

As depicted in Fig. 5, all samples show a dominant absorption structure centered at 0.63 eV.

For estimated high $R_{\text{NH}_3:\text{TMI}}$ precursor ratios (#31L \rightarrow #30L \rightarrow #22L) the absorption edge shifts downwards from an estimated 1.5 eV to approximate 1.0 eV, with absorption peaks / shoulders at 0.87 eV, 1.1 eV and 1.3 eV. For sample #24L_A the absorption edge is shifted below 0.9 eV and sample #25L_C suggest already an overall shifted absorption edge around 0.7 eV. The absorption peak centered at 0.63 remains in its strength.

The development of the absorption structures for these five samples suggest that the observed absorption edge shift from 1.5 eV down to below 0.7 eV is caused by a series of absorption structures, centered around 1.3 eV, 1.1 eV, and 0.87 eV. The appearance and strength of these

absorption centers correlate / coincide with the reduction of the molar ammonia to TMI precursor flow ratio, suggesting a close correlation between precursor ratio and the stoichiometry of the deposited layers.

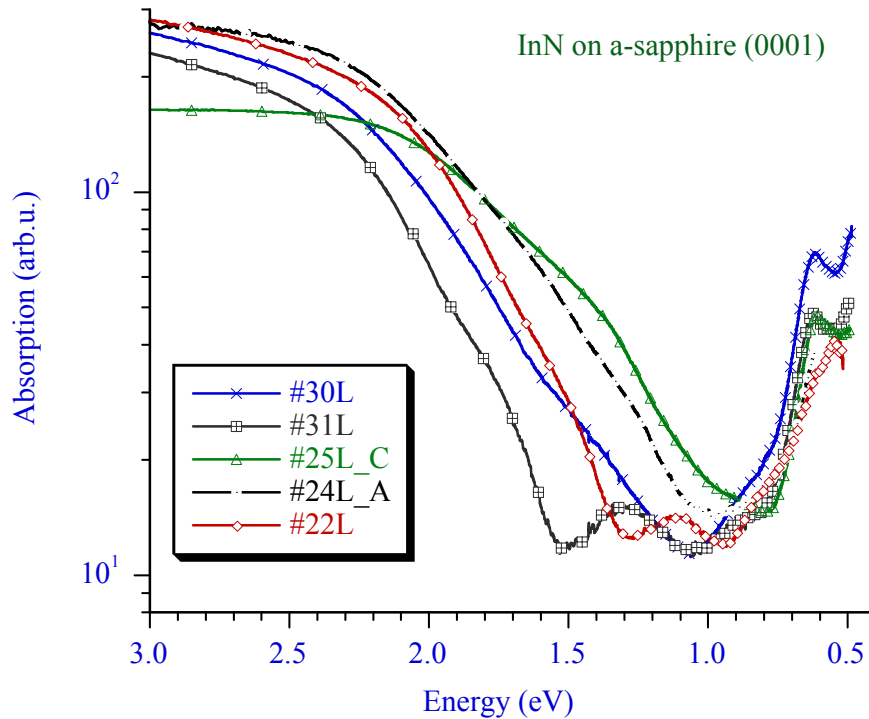


Figure 5:
Shift of absorption edge for five characteristic InN samples grown with different ammonia to TMI ratio.

4. CONCLUSION

For the growth of InN and related materials we introduced the first high-pressure CVD reactor capable of operating at pressures of up to 100 bar. The growth of InN has been explored in the laminar flow regime, evaluating the growth parameter for reactor pressures in range of 10 to 15 bars, gas flow velocities from 20 to 50 cm·s⁻¹, and molar ammonia to TMI ratios between 200 to 8000. High quality InN layers were achieved for growth temperatures in the range of 830°C to 850°C.

The optical InN layer characterization results indicate that the shift of the absorption edge from 1.5 eV down to approximate 0.7 eV may be caused by the appearance of several absorption centers, which origin is not clear at present. The initial results suggest that the molar ammonia to TMI flow ratio under HPCVD conditions is below 200, which is due to the efficient cracking of the nitrogen precursor at the high reactor pressure and high growth temperature. Further studies varying the ammonia to TMI flow ratio, the center flow velocity, and the growth temperatures will be needed to access the optimum growth window. The initial results demonstrate that the high-pressure CVD approach will allow the exploration of indium rich In_{1-x}Ga_xN and In_{1-x}Al_xN alloys and heterostructures. Even higher processing temperatures can be explored by further increasing the reactor pressure.

We also introduced principle angle reflectance spectroscopy (PARS) and demonstrated that PARS and LLS are able to follow the film growth process with sub-monolayer resolution, which will be an important tool for engineered nano-scale device structures. The link between the surface sensitive

PARS response to the real-time gas phase analysis (UVAS) allows to establish a comprehensive growth/flow model that will provide crucial insights in the gas phase decomposition kinetics, surface chemistry processes, and the film growth process at high pressures. Such a reactor model will be essential for the exploration of high-pressure process parameters that lead to turbulent flow conditions.

8. ACKNOWLEDGMENTS

This work was supported by NASA grant NAG8-1686 and GSU-RPE. M. S. gratefully acknowledges the support of the Alexander von Humboldt-foundation.

REFERENCES

- 1 S. Nakamura, *Jpn. J. Appl. Phys.* **30**, L1705 (1991).
- 2 S. Nakamura, M. Senoh, S. Nagahama, N. Iwasa, T. Yamada, T. Matsushita, H. Kiyoku, Y. Sugimoto, T. Kozaki, H. Umemoto, M. Sano, and K. Chocho, *Appl. Phys. Lett.* **73**(6) pp. 832-834 (1998).
- 3 S. Nakamura, M. Senoh, S. Nagahama, N. Iwasa, T. Yamada, T. Matsushita, H. Kiyoku, Y. Sugimoto, T. Kozaki, H. Umemoto, M. Sano and K. Chocho, *Appl. Phys. Lett.* **72**(16) pp. 2014-2016 (1998).
- 4 K. S. A. Butcher, M. Wintrebert-Fouquet, P. P.-T. Chen, T. L. Tansley, H. Dou, S. K. Shrestha, H. Timmers, M. Kuball, K. E. Prince, and J. E. Bradby, *J. Appl. Phys.* **95**(11) pp. 6124-6128 (2004).
- 5 K.S.A. Butcher and T.L. Tansley, *Superlattices and Microstructures* **38**(1), pp. 1-37 (2005).
- 6 A. G. Bhuiyan, A. Hashimoto, and A. Yamamoto, *J. Appl. Phys.* **94**(5), pp. 2779-2808 (2003).
- 7 V.Yu. Davydov, A.A. Klochikhin, V.V. Emtsev, D.A. Kurdyukov, S.V. Ivanov, V.A. Vekshin, F. Bechstedt, J. Furthmüller, J. Aderhold, J. Graul, A.V. Mudryi, H. Harima, A. Hashimoto, A. Yamamoto, E.E. Haller, *Physica Status Solidi B*, **234**(3) pp. 787-795 (2002).
- 8 V. Yu. Davydov and A. A. Klochikhin, *Semiconductors* **38**(8), pp. 861-898 (2004).
- 9 B. Monemar, P.P. Paskov and A. Kasic, *Superlattices and Microstructures* **38**(1) pp. 38-56 (2005).
- 10 N. Dietz, S. McCall, K.J. Bachmann, *Proc. Microgravity Conf. 2000*, NASA/CP-2001-210827, pp. 176 -181 (2001).
- 11 "Indium-nitride growth by HPCVD: Real-time and ex-situ characterization," N. Dietz, book chapter in "GaN-based Materials: Epitaxy and Characterization", ed. Z.C. Feng, Imperial College Press (ICP) pp. 1-31 (2005).
- 12 B. H. Cardelino, C. E. Moore, S. D. McCall, C. A. Cardelino, N. Dietz, K.J. Bachmann, CAITA-2004, Purdue University, June 2004, ISBN 86-7466-117-3 (2004).
- 13 V. Woods, H. Born, M. Strassburg and N. Dietz, *J. Vac. Sci. Technol. A* **22**(4), pp. 1596 - 1599 (2004).
- 14 N. Dietz, M. Strassburg and V. Woods, *J. Vac. Sci. Technol. A* **23**(4) pp. 1221-1227 (2005).
- 15 N. Dietz, V. Woods, S. McCall and K.J. Bachmann, *Proc. Microgravity Conf. 2002*, NASA/CP-2003-212339, pp. 169 -181 (2003).
- 16 N. Dietz, *Materials Science and Engineering B* **87**(1), pp.1 - 22 (2001)
- 17 T.L. Tansley and C.P. Foley, *J. Appl. Phys.* **59**(9) pp. 3241-4 (1986).
- 18 K. Osamura, S. Naka, and Y. Murakami, *J. Appl. Phys.* **46**(8) pp. 3432-3437 (1975).
- 19 Akihiro Wakahara and Akira Yoshida, *Appl. Phys. Lett.* **54**(8) pp. 709-711 (1989).
- 20 JCPDS International Centre for Diffraction Data file No 76-0152